Journal of

INTELLIGENT MATERIAL SYSTEMS *and* STRUCTURES

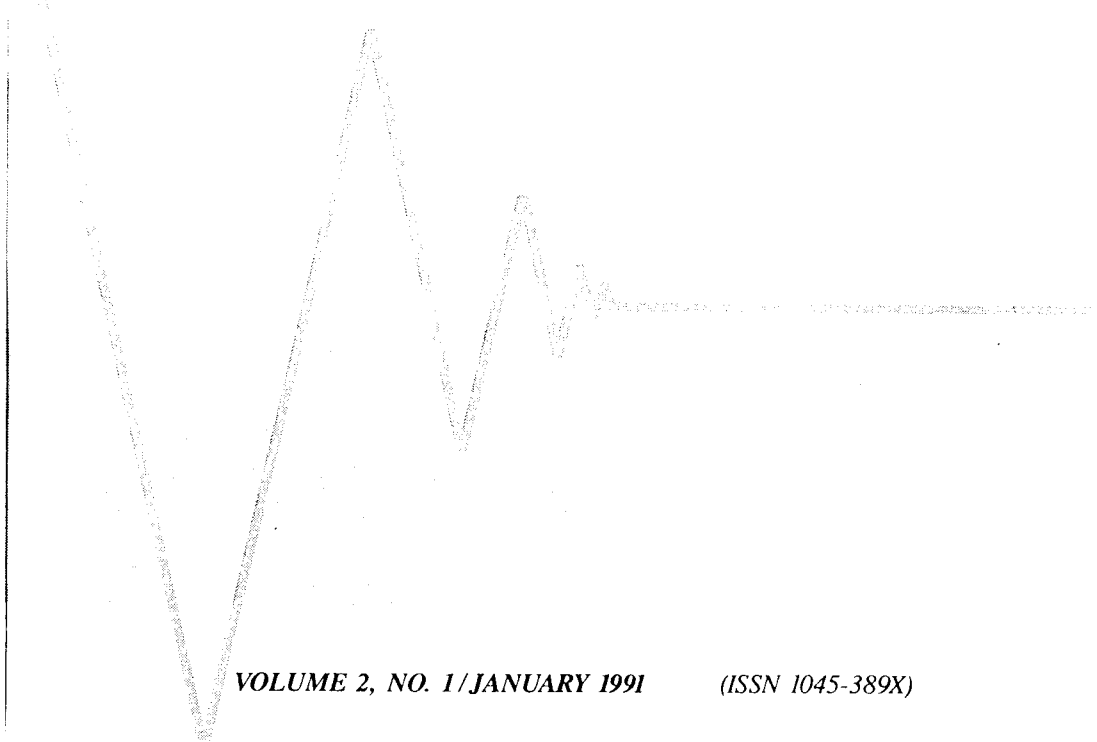

VOLUME 2, NO. 1/JANUARY 1991 *(ISSN 1045-389X)*

In this issue

Modeling of Finite-Length Spatially-Distributed Induced Strain Actuators for Laminate Beams and Plates

BOR-TSUEN WANG AND CRAIG A. ROGERS
Center for Intelligent Material Systems and Structures
Department of Mechanical Engineering
Virginia Polytechnic Institute and State University
Blacksburg, Virginia 24061-0238

ABSTRACT: A model for laminate beams and plates with attached or embedded finite-length spatially-distributed induced strain actuators has been formulated and is presented. A conservation of strain-energy model was developed by equaling the applied moment on the cross section of the edges of actuators to determine the induced linear strain distribution and the equivalent axial force and bending moment induced by the actuators. Results show that the strain-energy model for a thin laminate beam agrees well with the pin-force model. In addition, more general conditions were included in this work; for example, multiple actuators can be embedded in any layer of laminate. The concept of the conservation of strain-energy model for beams was also extended to a two-dimensional problem—plates. Classical laminate plate theory for spatially-distributed induced strain actuators developed previously by the authors is revised here to include the use of the strain-energy model. This work also compares several developed models and a finite element formulation. A simple approach to the application of induced strain actuators to the vibration and noise control of laminate beams and plates is provided.

INTRODUCTION

"INTELLIGENT MATERIAL SYSTEMS and structures" integrated with distributed sensors and actuators, have provoked a great deal of interest in the area of vibration and noise control in recent years. Distributed induced strain actuators, such as piezoceramic materials, have been widely chosen to achieve active control in both structural vibration (Crawley and de Luis, 1987; Bailey and Hubbard, 1985; Fanson and Chen, 1986) and structural acoustics (Dimitriadis and Fuller, 1989a; Wang, Dimitriadis and Fuller, 1989, 1990a).

To fully understand induced strain actuators, a description of the mechanical coupling between the actuators and the structure is needed, and many people have been devoted to developing a model for the interaction between actuators and structures. Crawley and de Luis (1987) developed a static model for one-dimensional piezoceramic patches bonded to the surface or embedded into the body of beams. They showed that distributed actuators perfectly bonded result in two equivalent concentrated moments acting at the edges of an actuator patch. Recently, Im and Atluri (1989) proposed a refined model including the transverse shear and axial forces in addition to the bending moments induced by actuators. Dimitriadis, Fuller and Rogers (1989b) presented a two-dimensional model for piezoceramic patches ideally bonded to the top and bottom surfaces of a rectangular plate, and showed that the resultant moments induced by the piezoceramic patches were along the four edges of piezoceramic patches under the assumption of spherical pure bending. This generally agrees with previous results (Crawley and de Luis, 1987).

Tzou and Tseng (1990) developed a finite element formulation for the application of distributed actuators to flexible shells and plates and presented two case study examples, i.e., a piezoelectric micro-position device and the distributed vibration identification and control. Ha and Chang (1990) also used finite element analysis to simulate the mechanical and electrical responses of fiber-reinforced laminated composites with distributed piezoelectric actuators. Wang and Rogers (1990b) applied classical laminate plate theory (CLPT) for finite-length, spatially-distributed induced strain actuators to determine the equivalent force and moment induced by actuators. They showed that actuators can induce in-plane forces and line moments along four edges of the actuator's patch to the laminate and result in the coupling of laminate plate extension and bending.

In addition to the use of distributed induced strain actuators in vibration or noise control, the design of distributed induced strain actuators has been investigated with encouraging results. Lee (1987) applied the classical laminate plate theory to the design of piezoelectric laminate for bending and torsional modal control. His experimental results showed that PVDF or PVF_2 (polyvinylidene fluoride) actuators can generate plate bending and twisting independently or simultaneously, and PVDF is suitable for active damping control of a flexible structure. Lazarus and Crawley (1989) developed the pin-force and consistent-plate models for the design of induced strain actuators. Exact solutions can be found only for the unconstrained boundary conditions; however, they also employed the Ritz assumed mode method to solve the problems with other boundary conditions.

This paper addresses the development of a theoretical model to determine the equivalent force and moment induced by the spatially-distributed induced strain actuators attached to or embedded in laminate beams and plates. The strain-energy model (SEM) for a laminate beam was derived first for a one-dimensional case and then extended to a two-dimensional, laminate actuator-plate problem. The CLPT for induced strain actuators developed by Wang and Rogers (1990b) was revised by the use of the strain-energy model for laminate beams described below. The current approach compares favorably with several other modelling approaches. The cases of pure bending in the beam and plate were illustrated and compared to the pin-force model (Lazarus and Crawley, 1989), the spherical pure bending model (Dimitriadis, Fuller and Rogers, 1989b) and a finite element formulation (Robbins and Reddy, 1990).

1045-389X/91/01 0038–21 $6.00/0

THEORETICAL ANALYSIS

Strain–Energy Model for a Laminate Actuator-Beam

Figure 1 shows the arrangement and coordinates of an arbitrary laminate beam with attached or embedded, finite-length, spatially-distributed actuators. The laminate actuator-beam with a length, L, and a width, b, has n layers, and contains m embedded actuators with length, L_a, and width, b_a. The purpose here is to determine the equivalent axial force and bending moment induced by these actuators. The basic assumptions are as follow:

1. Utilization of Euler-Bernoulli beam theory
2. Ideal bonding between layers and actuators
3. Infinite beam with finite-length actuators, i.e., $L \gg L_a$
4. Linear strain distribution, as illustrated in Figure 2, due to an induced strain actuator
5. Conservation of strain energy associated with the actuator and the assumed linear strain distribution of the laminate structure

First, the k-th actuator, as shown in Figure 2, was considered to determine its induced axial force and bending moment. The free strain of the k-th actuator is:

$$\Lambda_k = \frac{d_{31}}{t_{a_k}} V_k \tag{1}$$

Furthermore, the induced strain of the beam by this actuator was assumed to be a linear distribution, as shown in Figure 2, and has a magnitude of $\epsilon_k^* = K_k \Lambda_k$

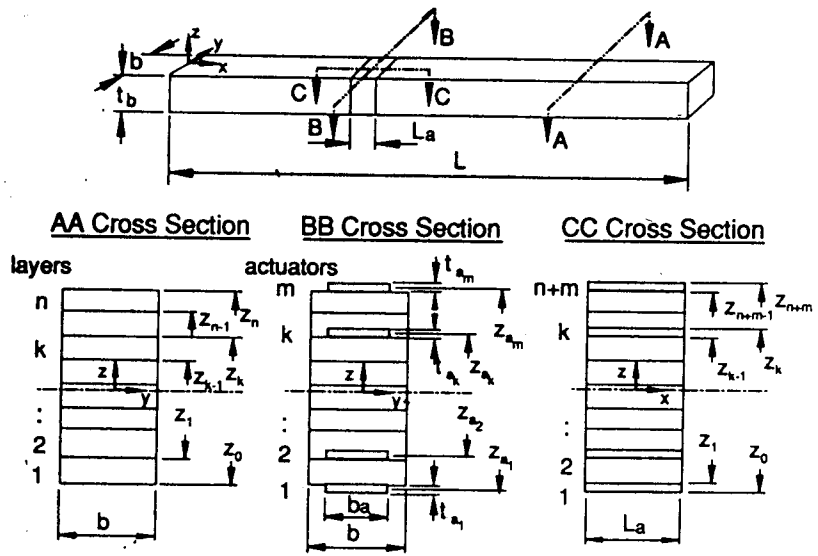

Figure 1. *Arrangement and coordinates of laminate actuator-beam.*

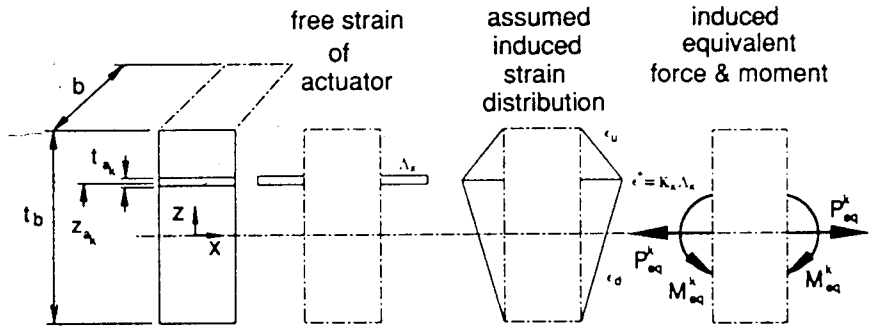

Figure 2. *Equivalent force and moment induced by the k-th actuator.*

at the actuator's location. Note that K_k is the unknown parameter. The distributed strain equations through the thickness of the beam above and below the actuator can be expressed as:

$$\epsilon_u = \frac{\epsilon_k^*}{\frac{t_b}{2} - z_{a_k}} \left(\frac{t_b}{2} - z \right) \tag{2}$$

and

$$\epsilon_d = \frac{\epsilon_k^*}{\frac{t_b}{2} + z_{a_k}} \left(\frac{t_b}{2} + z \right) \tag{3}$$

Because of the assumption of a linear strain distribution, the resultant actuator strain becomes the difference between the free strain of the actuator and the assumed strain. Therefore, the stress in the k-th actuator can be postulated to be uniform and expressed as

$$\sigma_{a_k} = E_{a_k}(\Lambda_k - \epsilon_k^*) = E_{a_k}(1 - K_k)\Lambda_k \tag{4}$$

The axial force and bending moment drawn by this stress can be found by:

$$P_{a_k} = t_{a_k} E_{a_k}(1 - K_k) b_a \Lambda_k \tag{5}$$

and

$$M_{a_k} = z_{a_k} t_{a_k} E_{a_k}(1 - K_k) b_a \Lambda_k \tag{6}$$

Next, from the assumed linear strain distribution, the stress distribution can

also be postulated. The induced equivalent bending moment can be obtained by the following integral through the beam thickness:

$$M_{eq}^{k} = \int_{-\frac{t_b}{2}}^{\frac{t_b}{2}} \sigma z b_a dz \tag{7}$$

where σ is the stress distribution due to the assumed strain. By substituting the strain Equations (2) and (3) into Equation (7) and integrating Equation (7), the equivalent bending moment becomes:

$$M_{eq}^{k} = \lambda_k K_k b_a \tag{8}$$

where

$$\lambda_k = \sum_{\substack{i=1 \\ p<k}}^{p} \frac{E_i}{\frac{t_b}{2} - z_{a_k}} \left[\frac{t_b}{4} (z_i^2 - z_{i-1}^2) - \frac{z_i^3 - z_{i-1}^3}{3} \right]$$

$$+ \sum_{\substack{i=p \\ p>k}}^{m+n} \frac{E_i}{\frac{t_b}{2} + z_{a_k}} \left[\frac{t_b}{4} (z_i^2 - z_{i-1}^2) + \frac{z_i^3 - z_{i-1}^3}{3} \right] \tag{9}$$

Based upon the assumption of the infinite beam, the equivalent bending moment induced by the single actuator must be equal to the bending moment induced by the assumed strain distribution. This statement is valid because of the conservation of strain energy. By setting Equations (6) and (8) equal, K_k can be found as:

$$K_k = \frac{z_{a_k} t_{a_k} E_{a_k}}{z_{a_k} t_{a_k} E_{a_k} + \lambda_k} \tag{10}$$

The equivalent axial force and bending moment induced by the k-th actuator can be found by substituting K_k into Equations (5) and (6):

$$P_{eq}^{k} = t_{a_k} E_{a_k} \left(\frac{\lambda_k}{z_{a_k} t_{a_k} E_{a_k} + \lambda_k} \right) b_a \Lambda_k \tag{11}$$

$$M_{eq}^{k} = z_{a_k} t_{a_k} E_{a_k} \left(\frac{\lambda_k}{z_{a_k} t_{a_k} E_{a_k} + \lambda_k} \right) b_a \Lambda_k \tag{12}$$

By superposition, the total equivalent axial force and bending moment induced by m actuators are:

$$P_{eq} = \sum_{k=1}^{m} P_{eq}^{k} \tag{13}$$

$$M_{eq} = \sum_{k=1}^{m} M_{eq}^{k} \tag{14}$$

Therefore, the resultant force and moment can be considered as external loads to the laminate beam. Im and Atluri (1989) demonstrated that actuators result in both the bending moment and the axial force simultaneously, except for the case of pure bending or extension in which the bending moment and axial force exist independently. This can also be seen in Table 1.

Strain-Energy Model for a Laminate Actuator-Plate

Wang and Rogers (1990b) developed the classical laminate plate theory for spatially-distributed induced strain actuators. Their work provides a theoretical basis for general application of induced strain actuators. However, results have

Table 1. Comparison between strain-energy and pin-force models.

case	strain-energy	pin-force
(1) pure bending	$M_{eq} = \frac{t_b^2 E_b}{6+\Downarrow} b \Lambda$	same $\left(\Downarrow = \frac{t_b E_b}{t_a E_a}\right)$
(2) pure extension	$P_{eq} = \frac{2 t_b E_b}{6+\Downarrow} b \Lambda$	$P_{eq} = \frac{2 t_b E_b}{2+\Downarrow} b \Lambda$
(3)	$P_{eq} = \frac{t_b E_b}{6+\Downarrow} b \Lambda$ $M_{eq} = \frac{t_b^2 E_b}{2(6+\Downarrow)} b \Lambda$	$P_{eq} = \frac{t_b E_b}{1+\Downarrow} b \Lambda$ $M_{eq} = \frac{t_b^2 E_b}{2(1+\Downarrow)} b \Lambda$
(4)	$P_{eq} = \frac{t_b E_b}{1+\Downarrow} b \Lambda$	same

indicated that this approach is most accurate for high actuator thickness to plate thickness ratios, and overestimates the force and moment induced by actuators for thin laminates. Therefore, the motivation here is to apply the previous results of the strain–energy model for a laminate actuator-beam to the laminate actuator-plate problem. For brevity, the complete derivation which was described in Wang and Rogers (1990b) is omitted here. Instead, only the extension to the previous work is presented. The total strains are shown as the sum of mechanical strains and induced actuator strains by Wang and Rogers (1990b):

$$\{\epsilon\} = \{\epsilon^m\} + \{\Lambda\} \tag{15}$$

Here, the actuator strains are redefined using the notation introduced in Equation (4):

$$\{\Lambda\} = \begin{bmatrix} \Lambda_x \\ \Lambda_y \\ \Lambda_{xy} \end{bmatrix} = \begin{bmatrix} \sum_{k=1}^{m} [H(z - z_k^a) - H(z - z_k^a)] \dfrac{(d_{31})_k}{z_k^a - z_k^a} V_k(1 - K_{k_x}) R_k(x, y) \\ \sum_{k=1}^{m} [H(z - z_k^a) - H(z - z_k^a)] \dfrac{(d_{32})_k}{z_k^a - z_k^a} V_k(1 - K_{k_y}) R_k(x, y) \\ \sum_{k=1}^{m} [H(z - z_k^a) - H(z - z_k^a)] \dfrac{(d_{36})_k}{z_k^a - z_k^a} V_k(1 - K_{k_{xy}}) R_k(x, y) \end{bmatrix} \tag{16}$$

Note that K_{k_x}, K_{k_y} and $K_{k_{xy}}$, the new terms not included in the previous work of Wang and Rogers (1990b), are defined similarly to K_k in Equation (10) except that λ_k should be replaced by λ_{k_x}, λ_{k_y}, $\lambda_{k_{xy}}$, respectively, and E_i in Equation (9) should be replaced by E_{i_x}, E_{i_y} and $E_{i_{xy}}$. The Heaviside function, $H(z - z_0)$, is defined as:

$$\begin{aligned} H(z - z_0) &= 1, \; z \geq z_0 \\ &= 0, \; z < z_0 \end{aligned} \tag{17}$$

and the generalized location function is defined as:

$$\begin{aligned} R_k(x, y) &= 1, \; (x_1)_k \leq x \leq (x_2)_k, (y_1)_k \leq y \leq (y_2)_k \\ &= 0, \text{ elsewhere} \end{aligned} \tag{18}$$

The equations of motion given by Wang and Rogers (1990b) remain the same

except for the changes of matrix $[E]$ and $[F]$. The i-th and j-th elements of $[E]$ and $[F]$ were redefined as:

$$\begin{aligned} E_{ij} &= \sum_{k=1}^{m} (\bar{Q}_{ij})_k^a (1 - K_{k_x}) V_k, \text{ if } j = 1 \\ &= \sum_{k=1}^{m} (\bar{Q}_{ij})_k^a (1 - K_{k_y}) V_k, \text{ if } j = 2 \\ &= \sum_{k=1}^{m} (\bar{Q}_{ij})_k^a (1 - K_{k_{xy}}) V_k, \text{ if } j = 3 \end{aligned} \tag{19}$$

$$\begin{aligned} F_{ij} &= \frac{1}{2} \sum_{k=1}^{m} (\bar{Q}_{ij})_k^a (1 - K_{k_x}) V_k (z_k^a + z_k^a), \text{ if } j = 1 \\ &= \frac{1}{2} \sum_{k=1}^{m} (\bar{Q}_{ij})_k^a (1 - K_{k_y}) V_k (z_k^a + z_k^a), \text{ if } j = 2 \\ &= \frac{1}{2} \sum_{k=1}^{m} (\bar{Q}_{ij})_k^a (1 - K_{k_{xy}}) V_k (z_k^a + z_k^a), \text{ if } j = 3 \end{aligned} \tag{20}$$

Note that K_{k_x}, K_{k_y} and $K_{k_{xy}}$, the k-th actuator induced strain constants, are functions of the material and physical properties of the laminate actuator-plate, and relate the interaction of layers and actuators.

EXAMPLE

Illustration of Actuator-Beam (Pure Bending)

Consider a beam with two actuators attached to the top and bottom of its surface symmetrically as shown in Figure 3, and activated 180° out of phase, i.e., $V_1 = -V_2$. The stresses of both actuators can be postulated as:

$$\sigma_{a_1} = E_a(-\Lambda + \epsilon^*) = -E_a(1 - K)\Lambda \tag{21}$$

and

$$\sigma_{a_2} = E_a(\Lambda - \epsilon^*) = E_a(1 - K)\Lambda \tag{22}$$

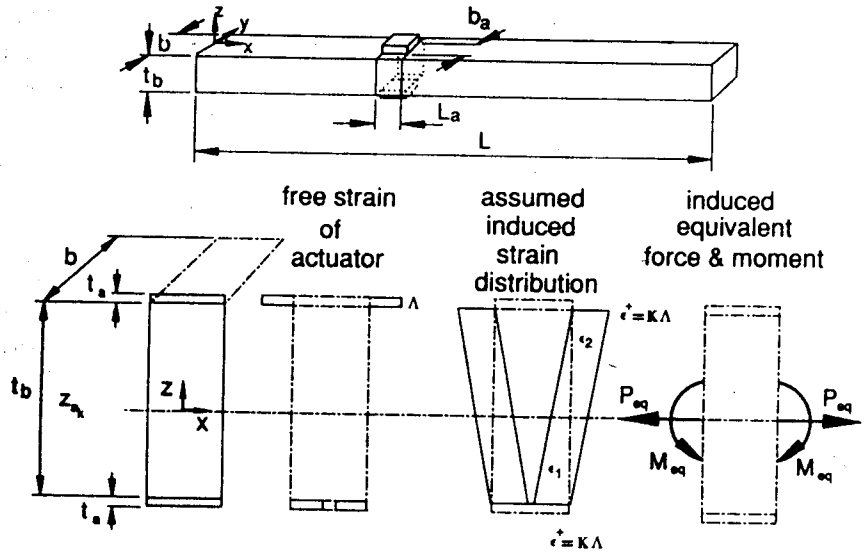

Figure 3. *Illustration of actuator-beam (pure bending).*

where $\Lambda = V_1 d_{31}/t_a$. Therefore, the axial force and bending moment induced by these two actuators are:

$$P_a = P_{a_1} + P_{a_2} = 0 \tag{23}$$

and

$$M_a = M_{a_1} + M_{a_2} = t_a E_a (1 - K) b_a \Lambda \tag{24}$$

Note that the sum of the axial forces by these two actuators is zero because the actuators were arranged symmetrically and activated 180° out-of-phase. As shown in Figure 3, if the assumed induced strain distributions, ϵ_1 and ϵ_2, are linear, then the equivalent bending moment drawn by these two assumed strain distributions can be derived as:

$$M_{eq} = \frac{t_b^2 E_b}{6} K b_a \Lambda \tag{25}$$

By setting Equations (24) and (25) equal, i.e., the conservation of the strain energy is maintained, K can be found as:

$$K = \frac{6}{6 + \Psi} \tag{26}$$

where

$$\Psi = \frac{t_a E_b}{t_a E_a} \tag{27}$$

Therefore, the induced equivalent bending moment can be determined by substituting Equation (26) into Equations (24) or (25):

$$M_{eq} = \frac{t_b^2 E_b}{6 + \Psi} b_a \Lambda \tag{28}$$

This result agrees with those of the pin-force model (Lazarus and Crawley, 1989) and the ideal bonding case (Crawley and de Luis, 1987) because, for the case of pure bending, all of these models have the same assumed linear strain distributions. Table 1 summarizes the results of several cases deduced from the strain-energy model and the pin-force model. Only for cases (1) and (4) do both models conclude the same equivalent bending moment and axial force. For other cases, they are somewhat different. This discrepancy is caused by the assumption of different types of strain distribution.

STATIC ANALYSIS

A cantilever beam, as shown on the top of Figure 4, is subjected to the actuation of a pair of piezoelectric patches attached symmetrically at the top and bottom of the beam and driven 180° out-of-phase. The piezoelectric actuation is equivalent to two concentrated moments, as indicated in Equation (28), with opposite signs acting on the two edges of the piezoelectric patches. The beam deflection can then be determined by classical beam theory.

For verification of the strain-energy model (SEM), a finite element code developed by Robbins and Reddy (1990) which utilizes generalized laminated plate theory (GLPT) was applied to obtain the static deflection of the beam. To compare the results, the relative error of the tip displacement of the cantilever actuator-beam is shown relative to the FEM results obtained by varying the ratio of the modulus to the thickness of the beam and actuators [Figures 4(a) and 4(b), respectively]. The results show that the error is generally less than 10% between the SEM and FEM. It is noted that for static analysis, the SEM overestimates the static response for low thickness ratios. However, it will also be shown that the SEM agrees well with the FEM for dynamic responses, because thickness effects become insignificant in dynamic analysis.

DYNAMIC ANALYSIS

To illustrate the utility of the model for dynamic analysis, a simply-supported actuator-beam harmonically excited by piezoelectric actuators in a pure bending

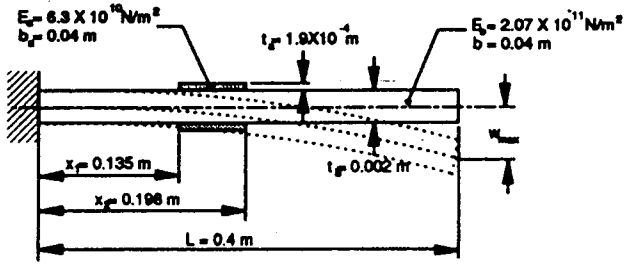

(a)

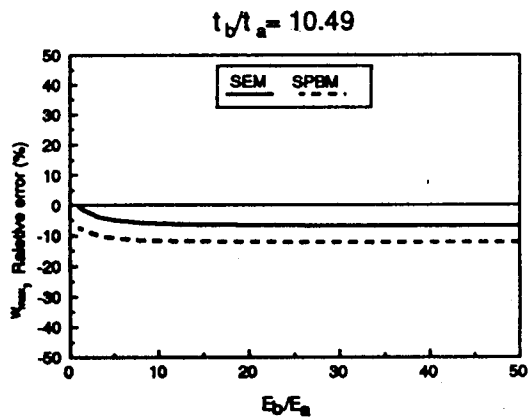

(b)

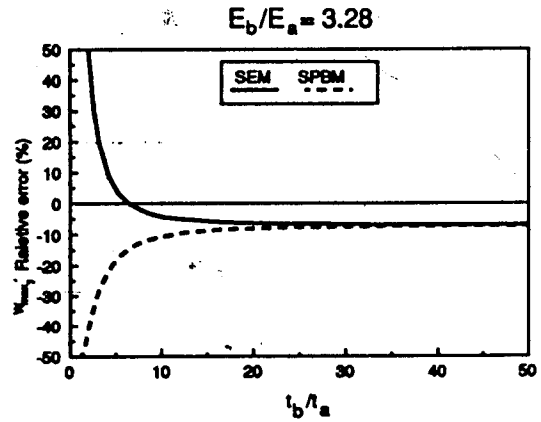

(c)

Figure 4. *Relative error of tip displacement respective to FEM.*

manner as described in the previous case study was considered. The lateral displacement of the beam can be described as:

$$w(x) = \sum_{m=1}^{\infty} W_m \sin \frac{m\pi}{L} x \tag{29}$$

where

$$W_m = \frac{P_m}{\varrho b t_b (\omega_m^2 - \omega^2)} \tag{30}$$

$$\omega_m = (m\pi)^2 \sqrt{\frac{E_b I}{\varrho b t_b L^4}} \tag{31}$$

and

$$P_m = \frac{2 M_{eq} m\pi}{L^2} \left(\cos \frac{m\pi}{L} x_1 - \cos \frac{m\pi}{L} x_2 \right) \tag{32}$$

Here, W_m is the modal amplitude, ω_m the natural frequency, I the moment of inertia, and P_m is the modal force for piezoelectric actuators which results in concentrated moments at both edges of the actuators.

For verification of the strain-energy model, the finite element code developed by Robbins and Reddy (1990) was applied to solve the modal amplitudes which were compared to the theoretical results from the SEM. Several numerical examples are presented. A simply-supported beam made up of steel with a length of 0.4 m and a thickness of 0.002 m (t_b/t_a = 10.49) or 0.0006 m (t_b/t_a = 3.15) with G-1195 piezoceramic patches attached to the top and bottom of the beam, as shown in the top of Figure 4, was considered. The material properties of the G-1195 piezoceramic patch are shown in Table 2, and the natural frequencies of the two beams are tabulated in Table 3.

Figure 5(a) shows the modal amplitude distributions and the steady-state modal

Table 2. Physical properties of G-1195 piezoceramic patch.

$d_{31} = d_{32} = 166 \times 10^{-12} \left(\frac{\text{m}}{\text{volt}}\right)$	$d_{36} = 0$
$\varrho_a = 7650 \left(\frac{\text{kg}}{\text{m}^3}\right)$	$E_a = 6.3 \times 10^{10} \left(\frac{\text{N}}{\text{m}^2}\right)$
$t_a = 1.905$ (mm)	$\nu_a = 0.28$

Table 3. Natural frequencies of simply-supported beam (rad/sec).

	t_b = 0.002 m (t_b/t_a = 10.49)		t_b = 0.0006 m (t_b/t_a = 3.15)	
Mode	Theoretical	FEM	Theoretical	FEM
1	182.6	181.1	54.8	54.9
2	730.6	728.1	219.2	220.6
3	1643.8	1649.2	493.2	502.4
4	2922.4	2968.5	876.7	907.9
5	4566.2	4708.9	1369.9	1399.7
6	6575.4	6849.1	1972.6	2087.8
7	8949.8	9531.2	2684.9	2814.6
8	11689.5	12666.4	3506.9	3755.2
9	14794.6	16451.4	4438.4	4807.5
10	18264.9	20633.8	5479.5	6039.5

response for piezoelectric actuators driven at ω = 400 rad/sec, a frequency between the first and second modes for the case of t_b/t_a = 10.49. The actuators can drive all modes, especially the first two. It is shown that the FEM predicts higher modal amplitudes than either the SEM or the spherical pure bending model (SPBM) (Dimitriadis, Fuller and Rogers, 1989b); however, the modal amplitudes generally agree with one another. The modal response is exhibited as a combination of the first and second modes.

Figure 5(b) shows the case of a driving frequency at ω = 700 rad/sec, a frequency very near the second mode. It is seen that the second mode is more efficiently excited than other modes. The FEM predicts a much higher amplitude for the second mode than for the others because the driving frequency is closer to the second natural frequency predicted by the FEM than to that predicted by the SEM. It should also be noted that the truncating error from the finite element formulation is unavoidable with the higher modes. Nevertheless, this truncating error is assumed small if large numbers of elements are used (40 elements were used here). In terms of steady state modal response, the FEM approach generally shows a 20% higher than the two analytical models. The reason has been discussed previously as the FEM predicts the higher modal amplitudes than the others. However, the trend of the steady state modal response generally agrees to each others, and the SEM gives higher modal responses than the SPBM.

For the low thickness ratios, i.e., t_b/t_a = 3.15, Figures 6(a) and 6(b) show the modal amplitude distribution and steady-state modal response for piezoelectric actuators driven at ω = 130 rad/sec, between the first and second modes, and ω = 210 rad/sec, near the second mode. It can be seen that the results of the SEM generally agree with those of the FEM; however, the SPBM underestimates the modal amplitudes. Therefore, the SEM is more favorable than the SPBM when the thickness ratio is low.

Illustration of Actuator-Plate (Pure Bending)

Consider a simply-supported, isotropic lamina with two actuators bonded to the top and bottom surfaces of a plate as shown in Figure 7, and activated 180° out of phase such that the actuators induce the pure bending of the plate. The bending equation can be derived as:

$$D\nabla^4 w + \rho h \frac{\partial^2 w}{\partial t^2} = C_0'' \Lambda \left(\frac{\partial^2 R}{\partial x^2} + \frac{\partial^2 R}{\partial y^2} \right) \tag{33}$$

where

$$D = \frac{Eh^3}{12(1 - \nu^2)} \tag{34}$$

$$C_0'' = t_a(h + t_a)(1 - K)\frac{E_a}{1 - \nu_a} \tag{35}$$

and K is defined in Equation (26). It is noted that the actuators result in equivalent

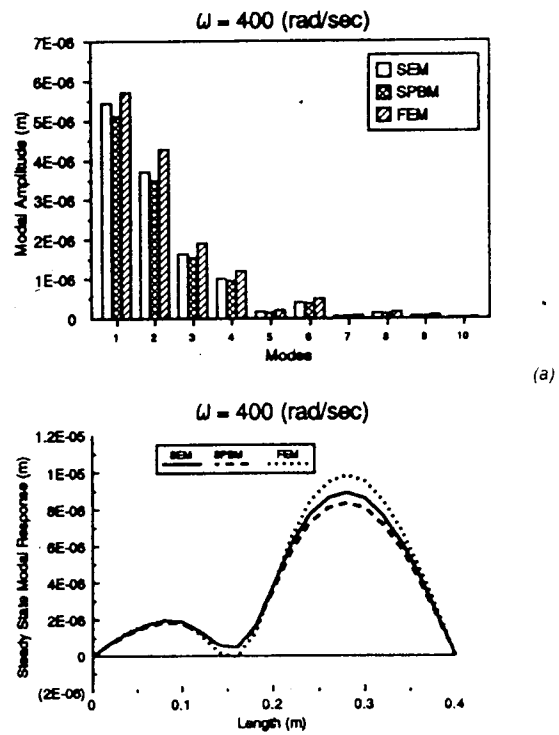

Figure 5. *Modal amplitude and modal response for h/t = 10.49, ω = 400 (rad/sec).*

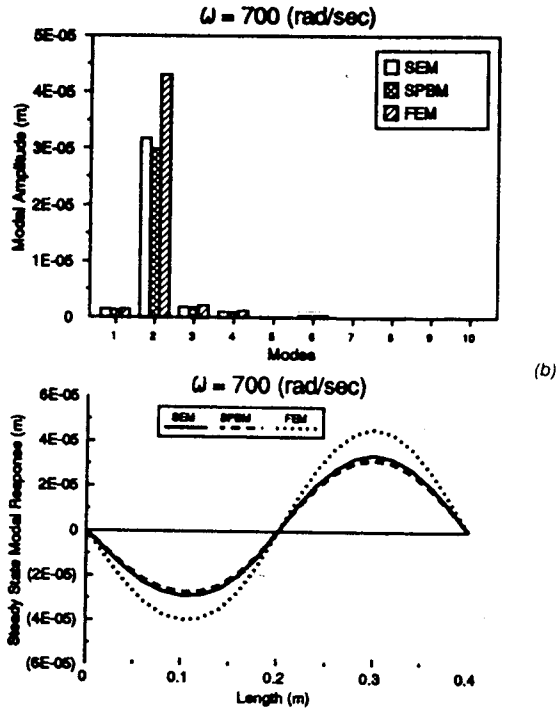

Figure 5 (continued). *Modal amplitude and modal response for h/t = 10.49, ω = 700 (rad/sec).*

line moments with a magnitude of C_0'' acting along the edges of the actuator's patch. The corresponding equation derived from the works of Dimitriadis, Fuller and Rogers (1989b) and Wang and Rogers (1990b) are the same except for the replacement of C_0'' by C_0 and C_0', respectively.

Figure 8 shows the induced line moment distribution obtained by varying the modulus ratio of the plate and actuator for different thickness ratios of the plate and actuator, while the physical properties of the piezoelectric actuators were assumed to be unchanged, i.e., t_a and E_a remain constant. As the modulus ratio increases, the line moment generally increases. That is to say, a stiffer plate with the same specified piezoelectric actuation will result in a higher line moment. However, the line moment will approach a constant when the modulus ratio is very large. For low modulus ratios, the variation of the line moment is more sensitive when the modulus ratio is increased, especially for those of low thickness ratios.

Figure 9 shows the line moment distribution obtained by varying the thickness ratio of the plate and actuator for various modulus ratios. It can be seen that the line moment increases as the thickness ratio increases; and it appears that there is a linear relationship between the line moment and the thickness ratio for high thickness and modulus ratios. The magnitude of the induced equivalent line moment is strongly relative to the plate thickness.

CONCLUSIONS

This paper presents the strain–energy model (SEM) for the laminate actuator-beam and plate which were based upon conservation of strain energy. An induced strain constant which relates the induced strain to the free strain of the piezoelectric actuator was derived. Therefore, the equivalent induced force and the line moment of the actuators can be determined. The theory presented herein provides a general approach of considerable utility for the application of induced strain actuators for noise and vibration control. Case study examples of pure bending for both beams and plates were presented, and a comparison between several models was made. This work is compared to several models including the pin-force model (Lazarus and Crawley, 1987), the spherical pure bending model (Dimitriadis, Fuller and Rogers, 1989b) and a finite element model developed by Robbins and Reddy (1990) and shows numerous advantages over other numerical models. Specifically, the SEM gives accurate results for a wide range of thickness ratios between actuators and beams. In addition, the SEM was also extended to two-dimensional problems, i.e., laminated plates. This work has revised the CLPT for spatially-distributed induced strain actuators (Wang and Rogers, 1990b) and is capable of predicting the equivalent axial force and bending mo-

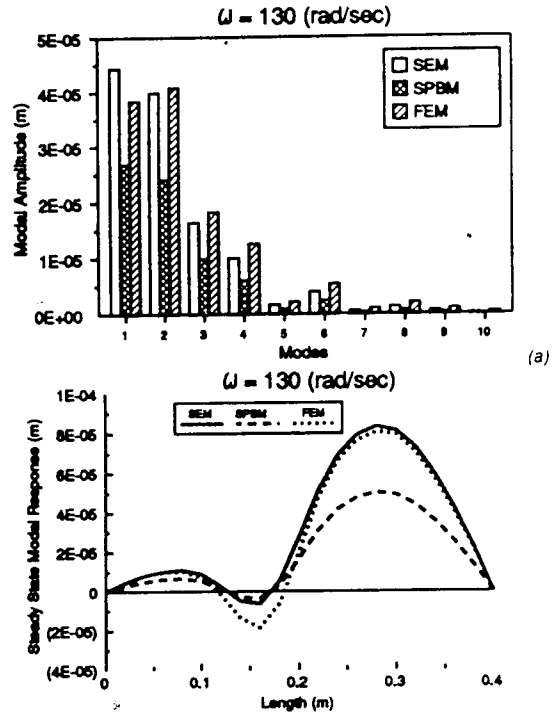

Figure 6. *Modal amplitude and modal response for h/t = 3.15, ω = 130 (rad/sec).*

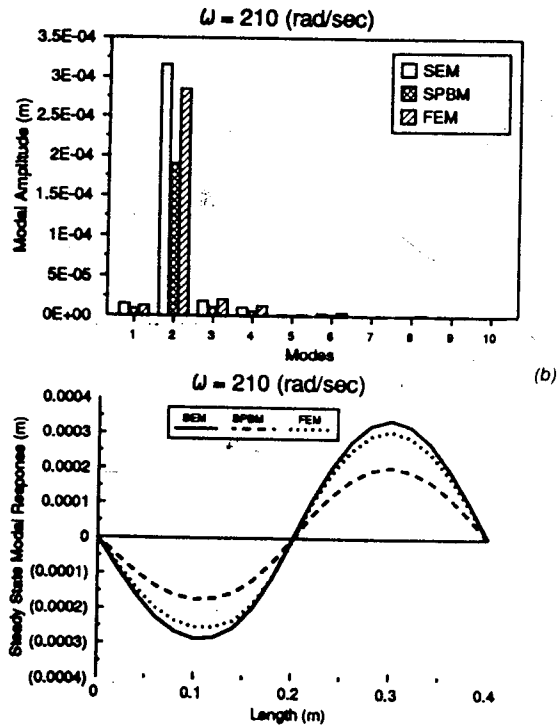

Figure 6 (continued). *Modal amplitude and modal response for h/t = 3.15, ω = 210 (rad/sec).*

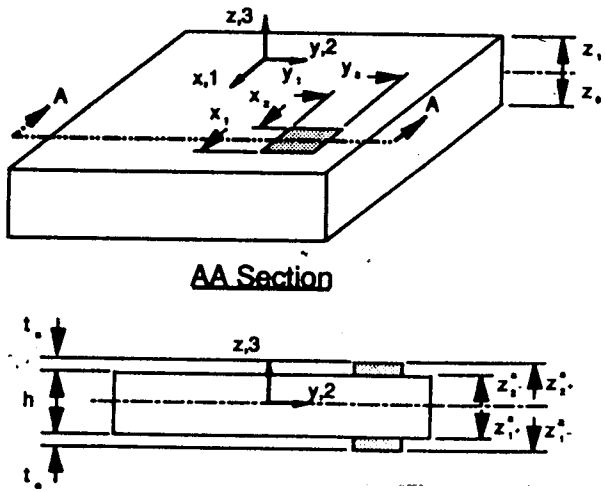

Figure 7. *Illustration of actuator-plate (pure bonding).*

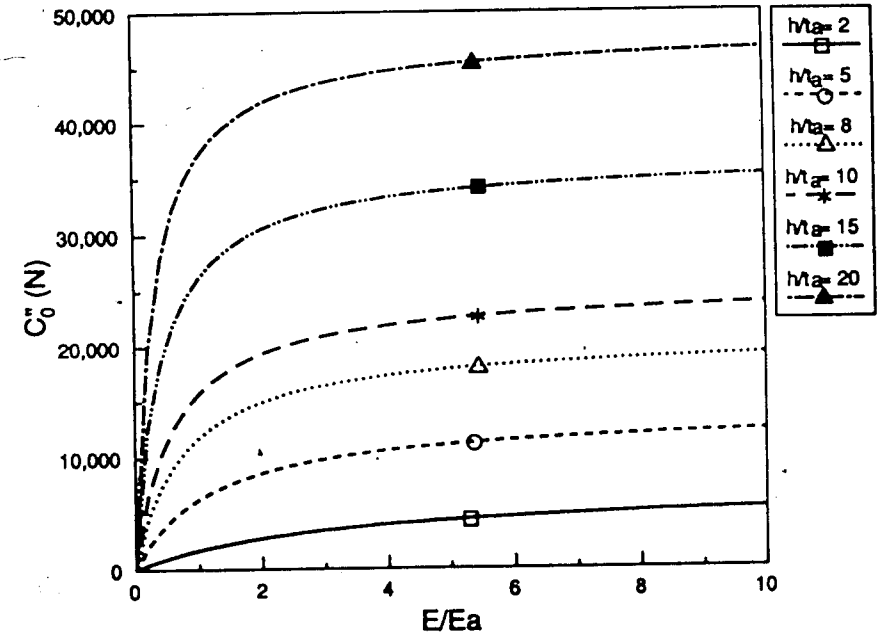

Figure 8. *Illustration of C_0'' by varying modulus ratio.*

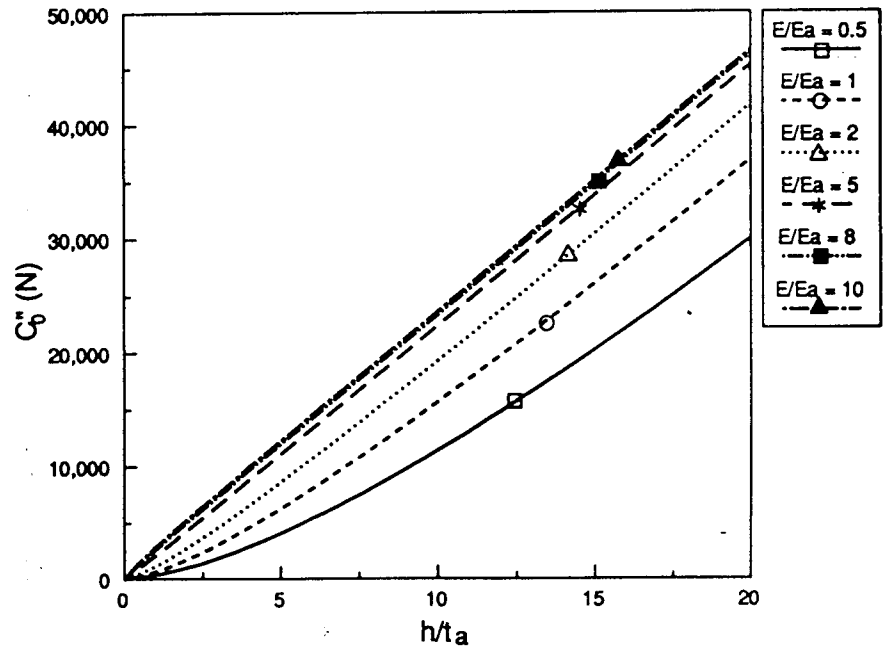

Figure 9. *Illustration of C_0'' by varying thickness ratio.*

ment induced by multiple spatially-distributed actuators. This work has been successfully applied to laminate beams or plates for active noise and vibration control.

ACKNOWLEDGEMENT

The authors wish to express their gratitude to Don Robbins and Professor J. N. Reddy in the Department of Engineering Science and Mechanics for providing the finite element code to make this work complete. This work has been supported by the Office of Naval Research, Young Investigator Program, ONR N0014-88-K-0566, and ONR Grant N0014-88-K0721.

NOMENCLATURE

b	beam width
b_a	actuator width
C_0	material constant for pure bending (Dimitriadis, Fuller and Rogers, 1989b)
C_0'	material constant for pure bending (CLPT) (Wang and Rogers, 1990b)
C_0''	material constant for pure bending (strain-energy model)
D	flexural rigidity
$(d_{ij})_k$	piezoelectric strain coefficient for the k-th layer actuator patch
$[E]$	actuator extensional stiffnesses
E	Young's modulus of an isotropic plate
E_a	Young's modulus of actuator
E_i	Young's modulus of the i-th layer lamina for beam
$[F]$	actuator bending-twisting stiffnesses
$H(x - x_0)$	Heaviside function
h	thickness of laminate plate
h_k	thickness of the k-th layer lamina
I	moment of inertial of the beam
K_k	induced strain constant of the k-th actuator for beam
K_{k_x}, K_{k_y}, $K_{k_{xy}}$	induced strain constant of the k-th actuator for plate
L	length of beam
L_a	length of actuator
M_a	bending moment induced by single actuator
M_{eq}	equivalent bending moment induced by actuators
m	number of actuator patches
n	number of laminae
P_a	axial force induced by single actuator
P_{eq}	equivalent axial force induced by actuators
P_m	modal force induced by piezoelectric actuators
$(\bar{Q}_{ij})_k^*$	material properties of the k-th actuator in (x,y,z) coordinates
$R_k(x,y)$	generalized location function of the k-th actuator patch
t_a	thickness of actuator patch
t_b	thickness of beam

W_m	modal amplitude for beam lateral vibration
w	plate lateral displacement
$(x_c)_k$, $(y_c)_k$	position coordinates of actuator patches
(x,y,z)	the laminated plate coordinates
V_k	voltage applied to the k-th actuator patch
z_k	thickness coordinate of the k-th layer
z_k^a, z_k^a	coordinate of actuator patch in z-direction
z_{a_k}	coordinate of the k-th actuator
∇	divergence operator
$\{\epsilon\}$	total strain vector in (x,y,z) coordinates
$\{\epsilon^m\}$	mechanical strain vector
ϵ_a	assumed linear strain distributions below the actuator's location
ϵ_a	assumed linear strain distributions above the actuator's location
ϵ_k^*	magnitude of the assumed linear strain at the actuator's location
$\{\Lambda\}$	actuator strain vector
Λ_x, Λ_y, Λ_{xy}	actuator normal and shear strain
Λ_k	free normal strain of the k-th actuator
λ_k	a force function for the k-th actuator
ν	Poisson ratio of plate
ν_a	Poisson ratio of actuator
ϱ	equivalent density of laminate
σ	assumed stress distribution
σ_{ii}	normal stress
Ψ	nondimensional ratio of physical properties of beam and actuator
ω_m	natural frequency of beam

Subscripts

a	actuator
b	beam
k	k-th layer

REFERENCES

Bailey, T. and J. E. Hubbard, Jr. 1985. "Distributed Piezoelectric Polymer Active Vibration Control of a Cantilever Beam", *AIAA Journal of Guidance and Control*, 8(5):605-610.

Crawley, E. F. and J. de Luis. 1987. "Use of Piezoelectric Actuators as Elements of Intelligent Structures", *AIAA Journal*, 25(10):1373-1385.

Dimitriadis, E. K. and C. R. Fuller. 1989a. "Investigation on Active Control of Sound Transmission through Elastic Plates Using Piezoelectric Actuators", AIAA paper 89-1062.

Dimitriadis, E. K., C. R. Fuller and C. A. Roger. 1989b. "Piezoelectric Actuators for Distributed Noise and Vibration Excitation of Thin Plates", *Proceeding of ASME Failure Prevention and Reliability Conference, Montreal*, pp. 223-233.

Fanson, J. L. and J. C. Chen. 1986. "Structural Control by the Use of Piezoelectric Active Members", *Proceedings of NASA/DOD Control-Structures Interaction Conference*, NASA CP-2447, Part II.

Ha, S. K. and F.-K. Chang. 1990. "Finite Element Modeling of the Response of Laminated Composites with Distributed Piezoelectric Actuators", *Proceedings of the AIAA/ASME/ASCE/AHS 31st Structures, Structural Dynamics and Materials Conference, Long Beach, CA, April 2-4, 1990*, Paper No. AIAA 90-1131.

Im, S. and S. N. Atluri. 1989. "Effects of a Piezo-Actuator on a Finitely Deformed Beam Subjected to General Loading", *AIAA Journal*, 27(12):1801-1807.

Lazarus, K. B. and E. F. Crawley. 1989. "Induced Strain Actuation of Composite Plates", GTL Report No. 197, Massachusetts Institute of Technology, Cambridge, Massachusetts.

Lee, C.-K. 1987. "Piezoelectric Laminates for Torsional and Bending Modal Control: Theory and Experiment", Doctoral Dissertation, Cornell University.

Robbins, D. H. and J. N. Reddy. 1990. "Finite Element Analysis of Piezoelectrically Actuated Beams", personal correspondence.

Tzou, H. S. and C. I. Tseng. 1990. "Distributed Dynamic Identification and Controls of Flexible Shells", *Proceedings of the AIAA/ASME/ASCE/AHS 31st Structures, Structural Dynamics and Materials Conference, Long Beach, CA, April 2-4, 1990*, Paper No. AIAA-90-1089.

Wang, B.-T., E. K. Dimitriadis and C. R. Fuller. "Active Control of Panel-Radiated Noise Using Multiple Piezoelectric Actuators", The 118th Meeting of Acoustical Society of America, St. Louis, Missouri, November 27-December 1, 1989.

Wang, B.-T., E. K. Dimitriadis and C. R. Fuller. 1990a. "Active Control of Structurally Radiated Noise Using Multiple Piezoelectric Actuators", *Proceedings of the AIAA/ASME/ASCE/AHS 31st Structures, Structural Dynamics and Materials Conference, Long Beach, CA, April 2-4, 1990*. Paper No. AIAA-90-1172.

Wang, B.-T. and C. A. Rogers. 1990b. "Laminate Plate Theory for Spatially Distributed Induced Strain Actuators", presented at the 5th US-Japan Laminate Composite Conference, submitted to *Journal of Composite Materials*.